Ecotoxicology and Environmental Safety 216 (2021) 112196

Contents lists available at ScienceDirect

Ecotoxicology and Environmental Safety

journal homepage: www.elsevier.com/locate/ecoenv

Arsenic accumulation and speciation in two cultivars of *Pteris cretica* L. and characterization of arsenate reductase Pc*ACR2* and arsenite transporter Pc*ACR3* genes in the hyperaccumulating cv. Albo-lineata

Marek Popov [a,b], Veronika Zemanová [c,d], Jan Sácký [a], Milan Pavlík [c], Tereza Leonhardt [a], Tomáš Matoušek [e], Antonín Kaňa [f], Daniela Pavlíková [d], Pavel Kotrba [a,*]

[a] Department of Biochemistry and Microbiology, University of Chemistry and Technology, Prague, Technická 3, 166 28 Prague, Czech Republic
[b] Department of Botany and Plant Physiology, Czech University of Life Sciences Prague, Kamýcká 129, 16500 Prague, Czech Republic
[c] Isotope Laboratory, Institute of Experimental Botany, The Czech Academy of Sciences, Vídeňská 1083, 14220 Prague, Czech Republic
[d] Department of Agro-Environmental Chemistry and Plant Nutrition, Czech University of Life Sciences Prague, Kamýcká 129, 16500 Prague, Czech Republic
[e] Institute of Analytical Chemistry, The Czech Academy of Sciences, Veveří 97, 602 00 Brno, Czech Republic
[f] Department of Analytical Chemistry, University of Chemistry and Technology, Prague, Technická 5, 166 28 Prague, Czech Republic

ARTICLE INFO

Edited by Paul Sibley

Keywords:
Arsenic species
Hyperaccumulating fern
Phytochelatin
Organoarsenicals
Arsenate reductase
Arsenite antiporter

ABSTRACT

Pollution and poisoning with carcinogenic arsenic (As) is of major concern globally. Interestingly, there are ferns that can naturally tolerate remarkably high As concentrations in soils while hyperaccumulating this metalloid in their fronds. Besides *Pteris vittata* in which As-related traits and molecular determinants have been studied in detail, the As hyperaccumulation status has been attributed also to *Pteris cretica*. We thus inspected two *P. cretica* cultivars, Parkerii and Albo-lineata, for As hyperaccumulation traits. The cultivars were grown in soils supplemented with 20, 100, and 250 mg kg^{-1} of inorganic arsenate (iAs^{V}). Unlike Parkerii, Albo-lineata was confirmed to be As tolerant and hyperaccumulating, with up to 1.3 and 6.4 g As kg^{-1} dry weight in roots and fronds, respectively, from soils amended with 250 mg iAs^{V} kg^{-1}. As speciation analyses rejected that organoarsenical species and binding with phytochelatins and other proteinaceous ligands would play any significant role in the biology of As in either cultivar. While in Parkerii, the dominating As species, particularly in roots, occurred as iAs^{V}, in Albo-lineata the majority of the root and frond As was apparently converted to iAs^{III}. Parkerii markedly accumulated iAs^{III} in its fronds when grown on As spiked soils. Considering the roles iAs^{V} reductase ACR2 and iAs^{III} transporter ACR3 may have in the handling of iAs, we isolated Albo-lineata Pc*ACR2* and Pc*ACR3* genes closely related to *P. vittata* Pv*ACR2* and Pv*ACR3*. The gene expression analysis in Albo-lineata fronds revealed that the transcription of Pc*ACR2* and Pc*ACR3* was clearly As responsive (up to 6.5- and 45-times increase in transcript levels compared to control soil conditions, respectively). The tolerance and uptake assays in yeasts showed that Pc*ACR*s can complement corresponding As-sensitive mutations, indicating that Pc*ACR2* and Pc*ACR3* encode functional proteins that can perform, respectively, iAs^{V} reduction and membrane iAs^{III} transport tasks in As-hyperaccumulating Albo-lineata.

1. Introduction

Being a ubiquitous trace metalloid toxin present in the environment, arsenic (As) is on the list of the 10 major substances of global concern (Oberoi et al., 2019). In humans the acute lethal dose ranges from 100 to 300 mg As, while chronic As exposures affect almost all organs, producing a range of health effects, including skin lesions, diabetes, lung and heart diseases, and cancer (NASEM, 2019; Oberoi et al., 2019; and references therein). Curiously enough, there are certain fungi (Braeuer et al., 2018; Larsen et al., 1998) and some ferns in which the As concentrations reach or even exceed 1000 mg kg^{-1} tissue dry weight (dwt). Chinese brake fern *Pteris vittata* L., the first identified As-hyperaccumulating plant, has been reported to accumulate in its fronds 22,630 mg kg^{-1} As (As concentrations in tissues hereinafter provided as in dry weight; dwt) when grown in soils containing 1500 mg kg^{-1} As and nearly 7000 mg kg^{-1} As growing in soils amended with

* Corresponding author.
E-mail address: pavel.kotrba@vscht.cz (P. Kotrba).

https://doi.org/10.1016/j.ecoenv.2021.112196
Received 29 September 2020; Received in revised form 19 March 2021; Accepted 24 March 2021
Available online 10 April 2021

400 mg kg^{-1} As (Ma et al., 2001). Further studies have identified more As hyperaccumulating fern species, including Cretan brake fern *Pteris cretica* L., and also non-hyperacumulating ones such as *P. ensiformis* L. or *P. semipinnata* L. (Claveria et al., 2019; Meharg, 2003; Rahman et al., 2018; Singh et al., 2010; Wang et al., 2012).

Different soils in the environment have varying background concentrations of As; it is generally present in soils in low concentrations (0.1–67 mg kg^{-1}) and the baseline soil As content typically ranges from 5 to 10 mg kg^{-1} (Cui and Jing, 2019 and references therein). In aerobic soils As mainly exists as inorganic arsenate (iAs^{V}), in anaerobic (e.g., paddy) soils as inorganic arsenite (iAs^{III}), and in both minor organoarsenical (OAs) compounds are present, such as mono-, di-, and trimethylarsenite/arsenate ($MA^{III/V}$, $DMA^{III/V}$, and $TMA^{III/V}$, respectively), which are produced from iAs by the soil microflora (Cui and Jing, 2019; Di et al., 2019). Of particular concern are anthropogenic activities, which can locally deposit iAs into soils at rates even exceeding 1 mg kg^{-1} $year^{-1}$ (Lebow et al., 2004). In Spain in 1998, a dam collapse at a retention mine pond, known as the Aznalcóllar disaster, flooded two rivers and affected ground water and 4286 ha of alluvial soil in which the As concentrations after reclamation have still remained ranging widely from 15 to nearly 800 mg kg^{-1} (Madejón et al., 2018).

The ability to hyperaccumulate As sparked the interest in *P. vittata* and other hyperaccumulating ferns as plants suitable for the phytoextraction of As from contaminated soils into aboveground, harvestable parts (Abou-Shanab et al., 2020; da Silva et al., 2018; Eze and Harvey, 2018; Fu et al., 2017; Jeong et al., 2014, 2015; Liu et al., 2018; Yang et al., 2020; and references therein), and thus into the As-related physiology in hyperaccumulating ferns (Abid et al., 2019; Fu et al., 2017; Han et al., 2017; Pavlíková et al., 2017, 2020; Yan et al., 2019; Zemanová et al., 2019, 2020; Zhang et al., 2017; and references therein). Prerequisites for efficient phytoextraction are, besides the mobilization of As in the soil, high As uptake and translocation rates, and the ability of the plant to deposit and tolerate high concentrations of As in its tissues (Li et al., 2016). Stemming from its chemical similarity with phosphate, physiologically irrelevant iAs^{V} is imported into the roots as a stowaway by using plasma membrane phosphate (Pi) transporters, and iAs^{III} mainly by using aquaporin channels (PvTIP4 aquaporin in *P. vittata*; He et al., 2016). The major known arsenate uptake transporters are in *P. vittata* represented by Pi deficiency- and As^{V}-inducible PvPht1;4 (Sun et al., 2020) and PvPht1;3 (DiTusa et al., 2016), the later expected also to be involved in the export of the substrates to the xylem sap for translocation. However, there are some Pi transporters that are apparently selectively discriminating for the transport of Pi, such as PvPht1;2 reported by Cao et al. (2018), or, as documented in model Arabidopsis plants, PvPht2;1, selectively transporting Pi to the chloroplasts, ameliorating As poisoning during photosynthesis (Feng et al., 2021).

The translocation of As into the aerial parts is then associated with the reduction of iAs^{V} to iAs^{III} by arsenate reductase(s); in the gametophytes of *P. vittata*, PvACR2 (Ellis et al., 2006) and newly discovered HAC (high As content) reductases PvHAC1 and PvHAC2 (Li et al., 2020) are instrumental in the iAs^{V} reduction. A study in sporophytes unveiled a bacterial-like As^{V} handling pathway with As^{V} being chemically trapped with phosphoglycerate by glyceraldehyde-3-phosphate dehydrogenase PvGAPC1 for transport by organic cation transporter PvOCT4 to endomembrane vesicles in which hydrolysis-born As^{V} becomes reduced to As^{III} by glutathione S-transferase PvGSTF1 with As^{III} eventually stored in vacuoles (Cai et al., 2019).

While the cellular detoxification of thiophilic iAs^{III} in roots and shoots of non-hyperaccumulating plants involves binding with phytochelatin peptides (PCs, possessing (γGlu-Cys) tandem repeats) with As^{III}-PC complexes eventually stored in vacuoles of both root and stem cells (Allevato et al., 2019; Wang et al., 2018; Liu et al., 2010), the dominant As storage form in the aerial parts of *Pteris* gametophytes is iAs^{III} (Han et al., 2017; Raab et al., 2004; Wan et al., 2018; Zhang et al., 2017). Unlike flowering plants employing PCs, *P. vittata* has at least two arsenite antiporters, PvACR3 and PvACR3;1, at its disposal to safely deposit iAs^{III} in frond vacuoles (Chen et al., 2017; Indriolo et al., 2010).

Our previous studies in *P. cretica* suggested marked difference in As accumulation in cv. Albo-lineata and Parkerii (Pavlíková et al., 2017, 2020; Zemanová et al., 2019, 2020). Here we detailed the As accumulation and speciation in both cultivars and show that while cv. Parkerii did not prove hyperaccumulating, the hyperaccumulation of As was confirmed in cv. Albo-lineata. The hyperaccumulation status of Albo-lineata prompted our efforts towards entering the investigation of molecular determinants in this fern, which lead to describing functional *ACR2* and *ACR3* genes, documenting their capacity to contribute to the As hyperaccumulation phenotype in this fern.

2. Material and methods

2.1. Plant material and growth conditions

The *P. cretica* L. gametophyte cultivars Albo-lineata and Parkerii were purchased at the 10–15 frond stage from garden center Tulipa Prague (Czech Republic) and grown in a greenhouse at 22–24 °C under natural-like controlled (as in Tulipa Prague) conditions with a 16 h day and 8 h night photoperiod cycles and relative humidity of 60%. The obtained ferns were allowed to acclimate in the experimental greenhouse for three days and then individually potted into 5 kg of haplic chernozem (pH_{KCl} 7.1) originating from the Prague-Suchdol site (Czech Republic, 50°8′8″ N, 14°22′43″ E; for physical and chemical properties of the soil see Zemanová et al., 2019). The soil was air dried and sieved with 2 mm mesh prior to amendment with 0.5 g of N, 0.16 g of P, and 0.4 g of K kg^{-1} dry soil wt (added as NH_4NO_3 plus K_2HPO_4) and supplementation with 20, 100, or 250 mg As kg^{-1} dry wt. To supplement the soil with As, it was thoroughly mixed with diluted Na_2HAsO_4 solution and left to mature for 10 d prior to use. The ferns in soils enriched with As were grown in parallel with those in the same soil without As supplement (Zemanová et al., 2019) and samplings were carried out after three different vegetation periods (30 and 90 d, and 185 or 158 d for cv. Albo-lineata or cv. Parkerii, respectively). For each cultivar, three individual ferns were grown per each As treatment and sampling period.

On the harvest day, the plants were separated into fronds and roots. The parts were weighted and those to be used in As analysis were oven-dried to a constant weight at 40 °C for 3 d. The parts to be used in the As speciation analysis or molecular analysis were frozen in liquid nitrogen, and then stored at −80 °C or fixed by freeze-drying and kept at −80 °C, respectively.

2.2. Arsenic analysis in plants

Total As concentrations were analyzed by inductively coupled plasma optical emission spectrometry (ICP-OES) using an Agilent 720 spectrometer (Agilent Technologies, Inc.). For the determination of total As in fronds and roots, the dried plant material (0.5 ± 0.05 g) was digested with 10 ml of a mixture of ultrapure HNO_3 and H_2O_2 (4:1, v/v; Lachner and Analytika, respectively) using an Ethos 1 apparatus (MLS GmbH). The analyses were conducted in triplicate and the quality of the mineralization and analytical procedures was tested with the certified reference material SRM 1573a – Tomato leaves from the US National Institute of Standards and Technology.

2.3. Arsenic speciation analysis

2.3.1. Size exclusion chromatography of extracted As

Plant tissues (1 g fresh weight of roots or fronds) were ground in liquid nitrogen with mortar and pestle and further disintegrated by using a One Shot Cell Disruptor (Constant Systems Ltd.) at 2.4 bar. Disrupted cells were extracted with 10 ml of 50 mM HEPES (pH 7.3) supplemented with EDTA-free cOomplete protease inhibitors (Roche Diagnostics) according to manufacturer's recommendation. Tissue

debris was removed by centrifugation at 30,000*g* and 4 °C for 10 min; the debris was digested with 1 ml 65% HNO_3 for 24 h, the sample volume was adjusted to 5 ml with distilled water. To determine the As extraction efficiency, As content of the sediment was measured by ICP-OES. The supernatant was further filtered on a PVDF syringe filter (0.45 μm; Teknokroma) and fractionated (2 ml) on a Superdex Peptide 10/300 GL column (GE-Healthcare) using a BioLogic DuoFlow FPLC system (BioRad) and 50 mM HEPES, 25 mM KNO_3 (pH 7.3) as a mobile phase at flow rate of 0.5 ml min^{-1}. Remaining filtrate to be used in PC analysis was stored at −80 °C. Ribonuclease A (GE Healthcare), ubiquitin (Sigma), and glutathione (Merck) were used as molecular mass standards. Arsenic contents in individual fractions from SEC were determined by ICP-OES.

2.3.2. Analysis of arsenicals

Arsenic species in fronds and roots were determined by selective hydride generation with pre-concentration by cryotrapping (HG-CT) and ICP mass spectrometry (ICP-MS) method. The method, semi-automated HG-CT-ICP-MS system employing an Agilent 7700x ICP-MS spectrometer with He collision cell (Agilent Technologies, Inc.), and system settings have been described in detail elsewhere (Currier et al., 2011; Matoušek et al., 2013). Homogenized frozen plant tissue (0.1 g fresh weight) was extracted with 5 ml of ice-cold 0.1% (v/v) formic acid (Lach-Ner, Ltd.) at 0 °C for 60 min, and the aliquots of slurry thus formed were used as samples. If needed, the slurries with high As content were further diluted with ice-cold 0.1% formic acid to keep iAs concentrations below 2 ng As ml^{-1}. For the measurements of iAs^{III}, 200 μl of the sample and 250 μl of water were injected into the system in which corresponding hydrides were generated at pH 6 selectively from the trivalent species. To measure the concentrations of iAs^{III} plus iAs^{V} species, the equal volumes of the sample and 250 mM L-cysteine (Merck) were combined and pre-reduction of As^{V} to As^{III} species was carried out for 60 min at room temperature before injection. The external iAs^{III}, MA^{III}, and DMA^{III} standards used for identification and peak area-based quantification were prepared in-house from As_2O_3 (Lachema), $Na_2CH_3AsO_3{\cdot}6H_2O$ (Chem Service, Inc.), and $H(CH_3)_2AsO_2$ (Strem Chemicals, Inc.), respectively, using L-cysteine as reductant (Matoušek et al., 2013). The calibration ranges were 0.5–2 ng As ml^{-1} for iAs^{III} and iAs^{V} standard, and 0.05–0.2 ng As ml^{-1} for methylated As^{III} species. TMA and a peak of unknown species were quantified against DMA^{III} calibration.

2.4. Phytochelatin analysis

The abundance of PCs was evaluated by gradient reverse phase high performance liquid chromatography (RP-HPLC) using an Agilent 1200 HPLC with an Agilent G1321A spectrofluorimetric detector (Agilent Technologies) and analytical Zorbax Eclipse XDB-C18 column (150 × 4.6 mm; 3.5 μm particles) as described previously (Osobová et al., 2011). Briefly, the sulfhydryls in the aliquots of the filtered tissue extracts or standard solutions were reduced by 50 μM trimethylphosphine (Sigma-Aldrich), fluorescent labeled in a reaction with 5 μM 7-fluorobenzofurazan-4-sulfonic acid (SBD-F; Sigma-Aldrich), and resolved on the column at 30 °C. The acetonitrile proportion in water (both with 0.1% [v/v] trifluoroacetic acid) during elution was 5–25% (v/v) linear gradient from 0 to 20 min, 25% to 70% from 20 to 25 min, 70% from 25 to 33 min, and 70% to 5% from 33 to 35 min. Fluorescence was scanned in multi-emission mode after excitation at 385 nm to facilitate spectrum shape-based confirmation of PC-SBDs; signal recorded at 515 nm was used in PC measurements. Data were analyzed by using ChemStation software (Agilent Technologies). Each of the three replicate cultured ferns was analyzed and custom-made PC2, PC3, PC4 (AnaSpec Inc.), and GSH (Merck) were used as external standards for identification and peak area-based quantification with the PCn calibration ranges of 0.1–200 μM.

2.5. PCR amplification and analysis of PcACR2 and PcACR3 genes and construction of plasmids

The chromosomal DNA and total RNA were isolated from 50 mg of freeze-dried fronds of plants grown in As_{100} soil for 90 d by using a NucleoSpin Plant II Kit (Macherey-Nagel) and an RNeasy Plant Mini Kit (Qiagen), respectively. An Oligotex mRNA Mini Kit (Qiagen) was used to obtain mRNAs from the total RNA and cDNA was synthesized from 1 μg of mRNA thus obtained by using an In-Fusion SMARTer Directional cDNA Library Construction Kit (Clontech). Double stranded cDNAs and genomic clones were produced by PCR that used Q5 High-Fidelity DNA polymerase (New England Biolabs); primary amplicons were maintained in pGEM-T Easy vector (Promega). Kits were used and routine RNA or recombinant DNA manipulations were performed following the manufacturers' instructions and standard protocols. Custom DNA sequencing (Eurofins Genomics) of plasmid inserts was done on both strands.

The chromosomal clone of Pc*ACR2* or full-length coding cDNA sequence were amplified by PCR in a reaction mixture containing pairs of gene specific primers designed based on the Pv*ACR2* mRNA sequence (GenBank accession no. DQ310370) and the genomic DNA (200 ng) or cDNA produced by the SMARTer Kit (1 μl) as template, respectively. The primers targeting sequences within the untranslated regions were 5'-CACGCATCAGCAGCAGCA-3' and 5'-GTCAAGCCATGATAGTTGCAAAGT-3', respectively. Similar homology-cloning approach, which employed Pv*ACR3* coding sequence information (GenBank accession no. HM559384) was used to obtain Pc*ACR3*. The in-coding-sequence primers 5'-ATGGAGAACTCAAGCGCGGAG-3' and 5'-CTAAACAGAAGGCCCCTTCCT-3' produced (from 200 ng of genomic DNA) the amplicon sequence used to design the primers allowing the determination of the 5' and 3' gene ends by using a GenomeWalker Universal Kit (Clontech). In the genome walking experiments, the 5 and 3 sequences of Pc*ACR3* gene were determined by using 5'-AGTATCAGACGGGTCGTTCCCATCAGC-3' (GSP1.1) plus 5'-AATGTCCAGGGCCATTTGCTGCTTCCG-3' (GSP2.1) with StuI library and 5'-ACAGCAGGCTCTTGCTGCCACAATAGG-3' (GSP1.2) plus 5'-CTCATAGAGGTGCCCGTGCTTCTCCTC-3' (GSP2.2) with *Pvu*II library, respectively.

The protein sequences deduced from the cDNAs were aligned with amino acid sequences of homologous proteins by Clustal 2.0.3 at UniProt (https://www.uniprot.org/blast/). The sequence analyses involved domain and residue conservancy scans at a PROSITE (Sigrist et al., 2013) and ConSurf (Ashkenazy et al., 2016) webservers, and transmembrane domain prediction at Phobius webserver (Käll et al., 2007). The 5′-region of Pc*ACR3* gene was analyzed for the presence of potential transcription factor binding sites by scanning against all plant motifs (99% similarity threshold, 90% returns all motifs) in the JASPAR CORE database (Mathelier et al., 2013). The Pc*ACR2* and Pc*ACR3* gene sequences were deposited in GenBank under the accession nos. MW027137 and MW027138, respectively.

The sequence information was used to design primers for the amplification of full-length coding cDNAs, which were inserted into *Bam*HI-treated yeast expression vector p426GPD by using an In-Fusion® HD Cloning Kit (Clontech). The vector p426GPD contains a constitutive glyceraldehyde-3-phosphate dehydrogenase (GPD) promoter, cytochrome *c* oxidase terminator, and *URA3* gene. The primers were 5'-*AAGCAGTGGTATCAA*ATGTCCTCGATTCCCAGCCT-3' and 5'-*CGGGGTACGATGAG*ATCAACATCCCCCGCAAAAGG-3' for Pv*ACR2* and 5'-*AAGCAGTGGTATCAA*ATGGCGAACTCCAGCGCGGA-3' and 5'-*CGG GGTACGATGAG*ACTAAGAAGTAGGCCACTTCC-3' for Pv*ACR3* (the primer extensions facilitating In-Fusion insertion of cDNA are italicized).

2.6. Functional complementation assays in S. cerevisiae

S. cerevisiae used for complementation assays were *arr2*Δ (YPR200c::kanMX4) and *arr3*Δ (YPR201w::kanMX4) mutants of BY4741 (*MAT*a *his3Δ1 leu2Δ0 met15Δ0 ura3Δ0*) strain used as the control; yeasts were purchased from Euroscarf (http://www.euroscarf.de). Yeasts transformed by p426GPD and its derivatives were selected and routinely grown at 30 °C on SD plates without uracil (SD medium: 0.7% [w/v]

Difco yeast nitrogen base, 2% [w/v] glucose, 0.005% adenine hemisulfate, and 0.003% [w/v] of each of L-histidine, and L-leucine, and L-methionine). For As tolerance plate assays, mid-log cultures of the *S. cerevisiae* transformants were adjusted to an optical density at 590 nm (OD_{590}) of 0.02, and 4 μl of serial dilutions were spotted on SD medium without metal or supplemented with sodium arsenate (*arr2*Δ transformants) or sodium arsenite (*arr3*Δ transformants). Arsenic toxicity assays in a liquid medium were initiated by inoculation of an arsenate/arsenite-containing SD medium with mid-log cultures to a turbidity of 0.4 McFarland units (equivalent to the OD_{590} of 0.1), and the culture growth was measured as cell suspension turbidity with a model DEN-1 densitometer (Bioscan, Riga, Latvia) after 48 h of cultivation. To determine the 50% inhibitory concentration ($IC_{50As,}$ the As concentration that reduced the culture turbidity by half), the data were adapted to the formula $T(c) = T(0)/\{1 + \exp[c\text{-}IC_{50As}]/b\}$, where c is the added As concentration, T(0) is the culture density reached in SD without As supplement and b is the slope of a sigmoidal dose-dependent curve (Hložková et al., 2016).

The As uptake assays in SD medium were initiated by adding the 20 or 50 μM sodium arsenite to 40 ml of the yeast cultures that reached OD_{590} of 1.6–1.8 and the cultures were further agitated for 1 h at 30 °C. The cells were then harvested by centrifugation at 4 000 × *g* and 25 °C for 2 min and washed twice with 30 ml of 50 mM phosphate buffer (pH 6.5) for 10 min. To determine the concentration of the accumulated As, the separated cells were digested with 0.75 ml of 65% nitric acid for 12 h and the sample volume was brought to 25 ml with distilled water. The cell debris was removed by 20 min centrifugation at 20,000 × *g* and the metal content of the supernatant was analyzed by ICP-MS using an ELAN DRC-e instrument (PerkinElmer). The ICP-MS system setup for the measurement of ^{75}As was as described previously (Beneš et al., 2019).

2.7. Quantitative real-time reverse-transcription PCR (qRT-PCR)

The analysis of Pc*ACR2* and Pc*ACR3* expression in the frond samples obtained from three plants after 90 d of growth in As-containing soils was performed by using iTaq Universal SYBR Green Supermix (Bio-Rad) as recommended by the manufacturer. The reaction contained 0.35 μM specific primers and 1 μl of cDNA (equivalent to 100 ng of the total RNA) prepared by using High Capacity Reverse Transcription Kit (Applied Biosystems) following the manufacturer's protocol. The concentration of RNA isolated from 50 mg of freeze-dried tissue using the RNeasy Plant Mini Kit was determined by measuring the absorbance at 260 nm, and its integrity was checked by formaldehyde agarose gel electrophoresis. The gene specific primer pairs were 5'-CTTCCGACCTCATCCGTCTGCG-3' plus 5'-CCATGACCCTGCAATGTGCCCA-3' for Ps*ACR2* and 5'-TGCTGATGGGAACGACCCGTC-3' plus 5'-TCCACACATACAGGTATCTATCG-3' for Pc*ACR3*. The qPCR analyses on three independent samples in two technical replicates were performed on MiniOpticon Real-Time PCR system (Bio-Rad); PCR conditions, data processing and primer specificity and DNA absence controls were performed as described previously (Sácký et al., 2014). The relative amount of Pc*ACR*s was calculated according to the $2^{-\Delta Ct}$ method using the expression level of the respective gene in As_0 fronds as a reference.

2.8. Statistics and data properties

Nonparametric Kruskal–Wallis test followed by Dunn's test were used for data evaluation as a prevention against potential platykurtosis caused by small group sizes. Scheirer–Ray–Hare test, two-factor extension of the Kruskal-Wallis test, was used for evaluation of factors interaction. Homoscedasticity of biomass yield was proven by Levene tests, but normality tested by Shapiro–Wilk tests showed deviations excluding the possibility of reliable use of ANOVA (the logarithmic transformation of data also does not lead to homoscedasticity and two-way ANOVA cannot be used). Scheirer–Ray–Hare test, two-factor extension of the Kruskal–Wallis test, was used for the evaluation of factor interaction. For most of other analytical data heteroscedasticity was observed, although the normality was proved. Therefore, the Welch's test followed by Games-Howell test was used. The Pearson's correlation coefficient and subsequent significance testing was used for correlation analysis. The significance level of p of 0.05 was used for all statistical tests. The Statistica 13.1 software (StatSoft, Inc., Tulsa, OK, USA) and Real Statistics Resource Pack software (Release 7.2, Charles Zaiontz) were used for the tests.

3. Results and discussion

3.1. Accumulation of As in P. cretica cultivars

A previous study has indicated that when grown in soil with a background As concentration of 16 mg kg^{-1} dry wt (As_0), the cv. Albo-lineata accumulates in fronds and roots significantly higher concentrations of As than cv. Parkerii (Zemanová et al., 2019; Table 1). To further compare the ability of these fern varieties to accumulate (and tolerate) As, they were grown in the same soil additionally supplemented with 20 (As_{20}), 100 (As_{100}) or 250 (As_{250}) mg As kg^{-1} dwt. In these conditions, the accumulation of As from the soils was time- and As concentration-dependent in both cultivars (Table 1), affecting also their frond (Fig. 1A) and root (Fig. 1B) biomass yields.

For *P. cretica* cv. Albo-lineata root biomass yield has not been significantly reduced between the 1st and 2nd sampling (2 months growth between samplings) for any of the As amended soils, except for the roots in the As_{250} exposure, where a 50% reduction of root biomass yield compared to As_0 exposure has been observed already during the 1st sampling (30 d after exposure, Fig. 1B), indicating a toxic effect of this level of As. On the other hand, As_{100} exposure did not show a significant reduction of the root biomass yield during the 1st and 2nd sampling, showing a strong tolerance of the root system of this cultivar to elevated As in soil. During the 3rd sampling (6 months of growth), both root and frond biomass yield has been decreased for As_{100} and As_{250} exposure (Fig. 1), which was also observed as abundant necrosis followed by drying of some fronds. Despite the visible differences in mean values, conservative Scheirer–Ray–Hare test did not prove any differences between frond biomass yield trends for individual As levels across sampling periods. On the contrary, root biomass yield trend across the sampling periods was significantly ($p < 0.05$) lower for As_{250} exposures.

Total As concentrations in the Albo-lineata cultivar were steadily rising in all tissues across all samplings on all soils (Table 1); furthermore, when translocation factor (TF, frond to root As concentration quotient) was calculated, it revealed a markedly increased As translocation to fronds on As_{100} and As_{250} soils, compared to the As_0 and As_{20} soils, especially during the later samplings. However, there was only a negligent difference between As_{100} and As_{250} TFs on 2nd sampling, and a comparably low TF difference on the 3rd sampling, indicating a translocation efficiency threshold. A root retaining capacity of approx. 1 mg As kg^{-1} was also indicated by the measurement of total As in roots, where there was no significant difference between the 1st, 2nd, and 3rd sampling for the As_{250} exposure (Table 1).

The Parkerii cultivar showed a stunted growth and decreased frond biomass yield already on As_0 and As_{20} compared to the Albo-lineata cultivar at all samplings (Fig. 1). At the time of the 3rd sampling (at 158 d in the case of Parkerii), the plants in As_{100} and As_{250} soils dried out almost completely, while plants from As_{20} soil showed a substantial necrosis of frond tips, reducing the non-necrotic biomass by 60% compared to the 1st sampling. Interestingly, root biomass yield has on average doubled between the 1st and 2nd sampling on all As amendments, even showing a comparable yield to Albo-lineata at As_{250} during the 2nd sampling. These root samples had also the highest measured total As content (124 ± 9.0 mg kg^{-1}, Table 1); however, this was 8 times lower than corresponding Albo-lineata samples. The highest As concentrations in Parkerii fronds were observed also at As_{250} soil during the 2nd sampling; however, as with the roots, the fronds contained nearly 19 times less total As compared to Albo-lineata samples from the same

Table 1
Total concentrations of arsenic (per dry weight) in fronds and roots of the two cultivars of *P. cretica* L. and calculated translocation factors (TF).

Cultivar	Soil	Fronds, sampling[a], and TF[b]			Roots and sampling[a]		
		1st (mg kg^{-1})	2nd (mg kg^{-1})	3rd (mg kg^{-1})	1st (mg kg^{-1})	2nd (mg kg^{-1})	3rd (mg kg^{-1})
Albo-lineata							
	As_0	6.3 ± 0.02[c] (0.89)	14.6 ± 0.5[c] (1.1)	17.1 ± 2.2[c] (0.62)	7.1 ± 0.7[c]	13.8 ± 5.1[c]	27.8 ± 1.4[c]
	As_{20}	28.7 ± 1.4 (0.31)	568 ± 15 (0.89)	476 ± 7.7 (1.4)	92 ± 4.2	410 ± 59	635 ± 33
	As_{100}	224 ± 26 (0.69)	2765 ± 141 (3.7)	5160 ± 379 (4.2)	326 ± 12	754 ± 34	1218 ± 9
	As_{250}	2108 ± 231 (2.1)	3668 ± 559 (3.7)	6444 ± 298 (4.9)	1009 ± 20	995 ± 184	1328 ± 20
Parkerii							
	As_0	< 3[c,d] (ND)	< 3[c,d] (ND)	3.1 ± 0.2[c] (0.48)	< 3[c,d]	< 3[c,d]	6.5 ± 3.5[c]
	As_{20}	5.1 ± 1.0 (> 1.7)	8.4 ± 1.4 (2.1)	9.2 ± 0.1 (> 3.1)	< 3[c]	6.5 ± 2.85	< 3[c]
	As_{100}	28.2 ± 1.2 (1.9)	85 ± 6.5 (3.9)	ND[e]	14.8 ± 1.0	21.6 ± 2.1	ND[e]
	As_{250}	122 ± 2 (2.6)	194 ± 10 (1.6)	ND[e]	47.7 ± 2.1	124 ± 9.0	ND[e]

[a] 1st sampling and 2nd saplings: 34 and 90 days, respectively; 3rd sampling of Albo-lineata and Pakerii: 185 and 158 days, respectively. Displayed are the average values obtained from 3 independent plants ± standard deviation.
[b] TF (frond to root As concentration quotient) calculated using mean values is shown in parentheses.
[c] See also Zemanová et al. (2019).
[d] Below limit of detection.
[e] ND, not determined.

conditions. Scheirer–Ray–Hare test did not prove any differences between fronds and roots biomass yield trends for individual As levels across sampling periods.

Taken together, these data clearly indicate markedly pronounced accumulation of As in Albo-lineata compared to Parkerii (up to more than two orders of magnitude in the same conditions) and also a better predisposition to tolerate As. Although absolute values of fronds and roots biomass yields are higher for Albo-lineata compared to Parkerii, no significant differences in fronds and roots biomass yield trends for individual As levels across sampling periods were not proved between cultivars. Observations in Albo-lineata, but not in Parkerii, are in agreement with previous reports on As accumulation in fronds of hyperaccumulating *P. cretica* cultivars in similar conditions (grown with 50–200 mg kg^{-1} As soil for up to 2 months; Eze and Harvey, 2018; Jeong et al., 2014; Meharg, 2003; Pavlíková et al., 2020; Zhang et al., 2017). Noteworthy, in an extensive study by Meharg (2003) in which he scored As accumulation capacity of 45 fern species has been Parkerii with its 2500 mg As kg^{-1} after 2 months in a soil amended with 100 mg kg^{-1} As attributed hyperaccumulator status, the property not seen here (Table 1).

It is generally accepted that the efficient translocation of As from roots is important for the hyperaccumulation of As in aboveground tissues and reducing the As toxicity in root cells (Singh and Ma, 2006). In spite of the hyperaccumulator status of Albo-lineata, when TF is considered as a measure of the ability to translocate As to aboveground parts, non-hyperaccumulating Parkerii shows more efficient translocation at lower soil As concentrations than Albo-lineata; TFs > 1 were in Parkerii, but not in Albo-lineata, observed after all, i.e. 1st, 2nd and 3rd, samplings from As_{20} soils and TF values > 1 can be seen with Parkerii in all, but As_0, soils (Table 1).

3.2. As speciation analyses and phytochelatin contents in As-exposed ferns

Studies in hyperaccumulating *Pteris* have revealed that tri- and pentavalent inorganic As species (iAs^{III} and iAs^{V}, respectively) represent the major As storage form, particularly in the plants exposed to and thus containing high concentrations of As (Chen et al., 2016; Tu et al., 2003; Zhang et al., 2017). To inspect the cellular As deposition forms in Albo-lineata and Parkerii and detect potential As-peptide (such as PC) complexes, the cell extracts obtained from the disintegrated fern tissues were first resolved by size exclusion chromatography (SEC). The extraction under the mild conditions of neutral pH, which liberated the majority of the total frond or root As (mean extraction efficiency was 86 ± 5%), was used to minimize the chance of As release from complexes if these were present in the cells. The SEC of the extracts from collected fronds and roots of Albo-lineata and Parkerii showed that As was contained in late eluting fractions corresponding to unbound arsenicals (Fig. 2A shows Albo-lineata fronds as example).

Considering free arsenicals were detected as dominant As species in the investigated ferns, the proportion of iAs^{III} and iAs^{V} and the presence of OAs species (OAs) was inspected in the ferns grown in As-containing soils for 90 d by using HG-CT-ICP-MS analysis. It has been documented that imported iAs^{V} is in *P. vittata* reduced mainly in the roots (Duan et al., 2005) and that translocated iAs^{III} dominates in the aboveground tissues of *P. vittata* and *P. cretica* cv. Nervosa as well (Chen et al., 2016; Zhang at al., 2017 and references therein). Indeed, nearly all As accumulated in the fronds of Albo-lineata was found as iAs^{III} while the iAs^{III}–to–iAs^{V} ratio in its roots gradually increased in As exposure-dependent manner (Fig. 2B) from 2:1 to more than 30:1. By contrast, the dominating form in the roots of Parkerii (e.g., 75% in As_0 and even 95% in As_{20} plants) was determined as iAs^{V} (Fig. 2B). It should be stressed, however, that these levels of iAs^{V} better resemble those seen reported from similar As exposures in *P. cretica* cv. Nervosa and hydroponically grown *P. vittata* with iAs^{V} present in 70–90% range (Chen et al., 2016; Zhang at al., 2017). Quite unusual appeared high iAs^{V} in the fronds of Parkerii, particularly in As_{250} plants, but also in As_0 plants in which low iAs^{V} reduction rate could not be attributed to As toxicity. Contrary to that, in fronds of As_{20} and As_{100} plants of the Parkerii cultivar, iAs^{III} was favored (Fig. 2B).

While the metabolism of As in plants seemingly does not involve biosynthesis of OAs such as MA, DMA, or TMA, ferns, like other plants, have certain capacity to accumulate these compounds (Tu et al., 2003) produced in the soils by indigenous microflora (Di et al., 2019). The probe to OAs levels of Parkerii using HG-CT-ICP-MS revealed measurable levels of OAs ($MA^{III/V}$, $DMA^{III/V}$, TMA and an unknown compound; Fig. 2C) in the samples extracted from roots (Table 2), but not fronds (data not shown). The overall concentrations of OAs apparently increased with increasing As in the soil but represented only minute portions of the total root As (e.g., 2.7%, 0.4%, 0.1%, and 0.1% of total As in 90 d exposures in As_0, As_{20}, As_{100}, As_{250}, respectively). The unknown compound was seen only in pre-reduced extracts, indicating it was As^{V}-containing OAs. The abundance of this OAs^{V} and the apparent prevalence of pentavalent forms well seen with all the inspected OAs in As_0 and As_{20} roots can be attributed to a substantially higher cellular toxicity of OAs^{III} (Di et al., 2019), with the oxidation of OAs^{III} representing a reasonable defense. It is worth noting, that the possibility that OAs were accumulated also in Albo-lineata cannot be excluded (rather it is likely) as extracts from this variety required high dilution before HG-CT-ICP-MS analysis and AOs might have been diluted out below

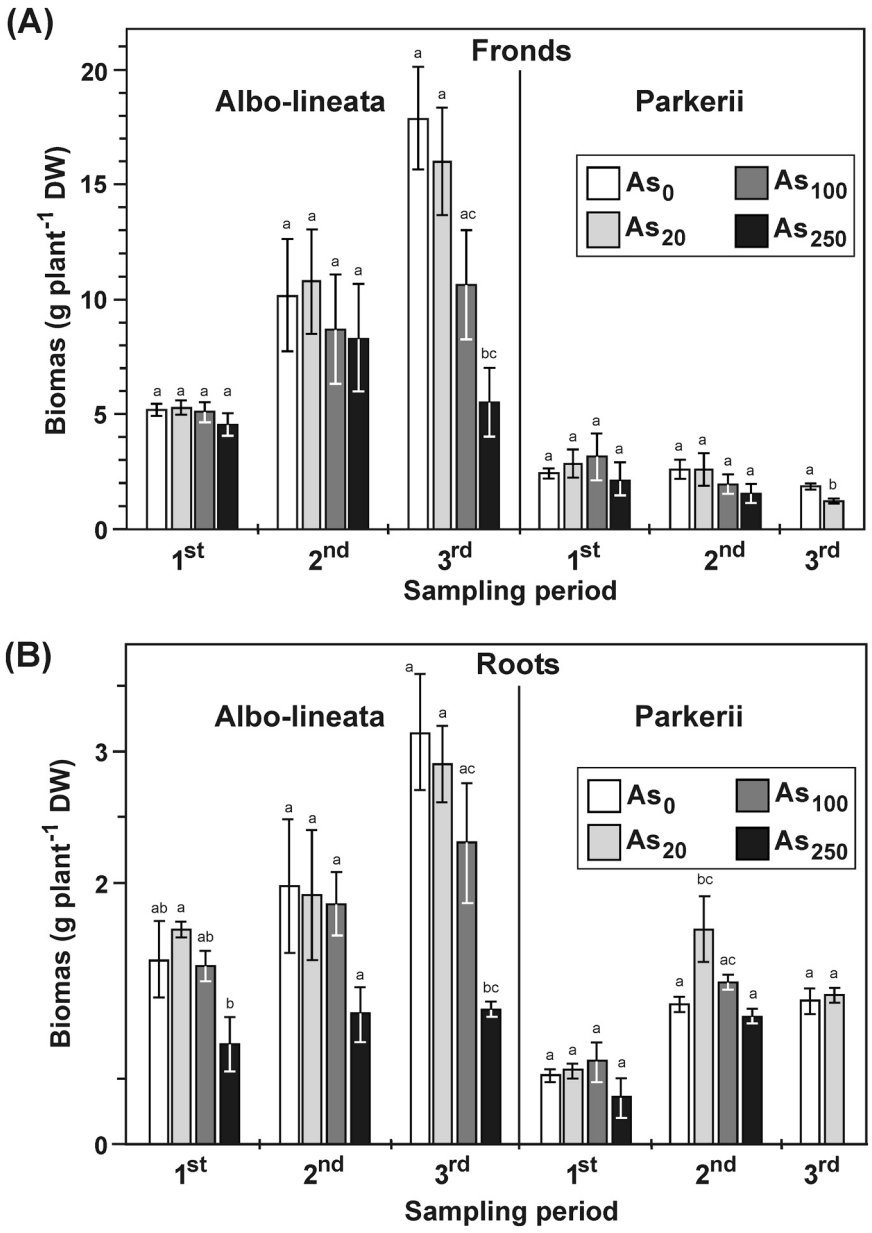

Fig. 1. Yields of fronds (A) and roots (B) of *P. cretica* cultivars. Albo-lineata and Parkerii after growth in As-amended soils as indicated. The plotted values represent the average of dry biomass from 3 independently grown plants ± standard deviation of the mean, and significant differences ($n = 3$; $p < 0.05$ Kruskall–Wallis test followed by Dunn's test) in a particular treatment are indicated by different letters above the bars.

method detection limit.

The absence of As peak(s) of a kDa range in SEC (Fig. 2A) indicated lacking or very low levels of As-PC complex(es) in the cells. Although iAs^{III} is on the list of ions inducing PC synthesis in plants (Most and Papenbrock, 2015), our observations corroborate with previous reports in *P. vittata* (Zhao et al., 2003) and *P. cretica* cv. Mayii (Raab et al., 2004) in which the PC levels would have bound theoretically 1–3% of the accumulated As. This is indeed markedly different from, e.g., flowering *A. thaliana* in which the elimination of glutamyl-cysteine synthetase involved in PC precursor GSH synthesis and PC synthase rendered the phenotype As-hypertensive (Wang et al., 2018 and references therein). To attest whether PCs were available in the ferns, the thiol-containing compounds extracted from the tissues from the first and second sampling were fluorescence labeled with sulfhydryl-specific SBD-F probe and analyzed by using RP-HPLC. Like in *P. vittata* and *P. cretica* (Raab et al., 2004; Zhao et al., 2003), both Albo-lineata and Parkerii showed PC2, but not PC3 or PC4 molecules. As documented in Fig. 2D, the levels of PC2 found in fronds and roots of plants from As-amended soils significantly increased with the increasing concentration of accumulated As. The correlations between the PC and As contents in fronds and roots, and between the PC and As levels in soil (As_{20}, As_{100}, As_{250}) were proved in some cases, but their occurrence appears to be random. Moreover, when the calculated molar concentrations are considered, the concentrations of accumulated As in the tissues of Albo-lineata and Parkerii exceeded the concentrations of PCs by three to four and two to four orders of magnitude, respectively (not shown).

3.3. *Identification of arsenate reductase ACR2 and arsenite transporter ACR3 in P. cretica cv. Albo-lineata*

The dominance of iAs^{III} in the tissues of arsenate-exposed Albo-lineata indicated efficient reduction of the imported iAs^{V} attributable to the cellular arsenate reductases, in *P. vittata* sporophytes identified as PvACR2 (Ellis et al., 2006), the ortholog of we investigated here, and

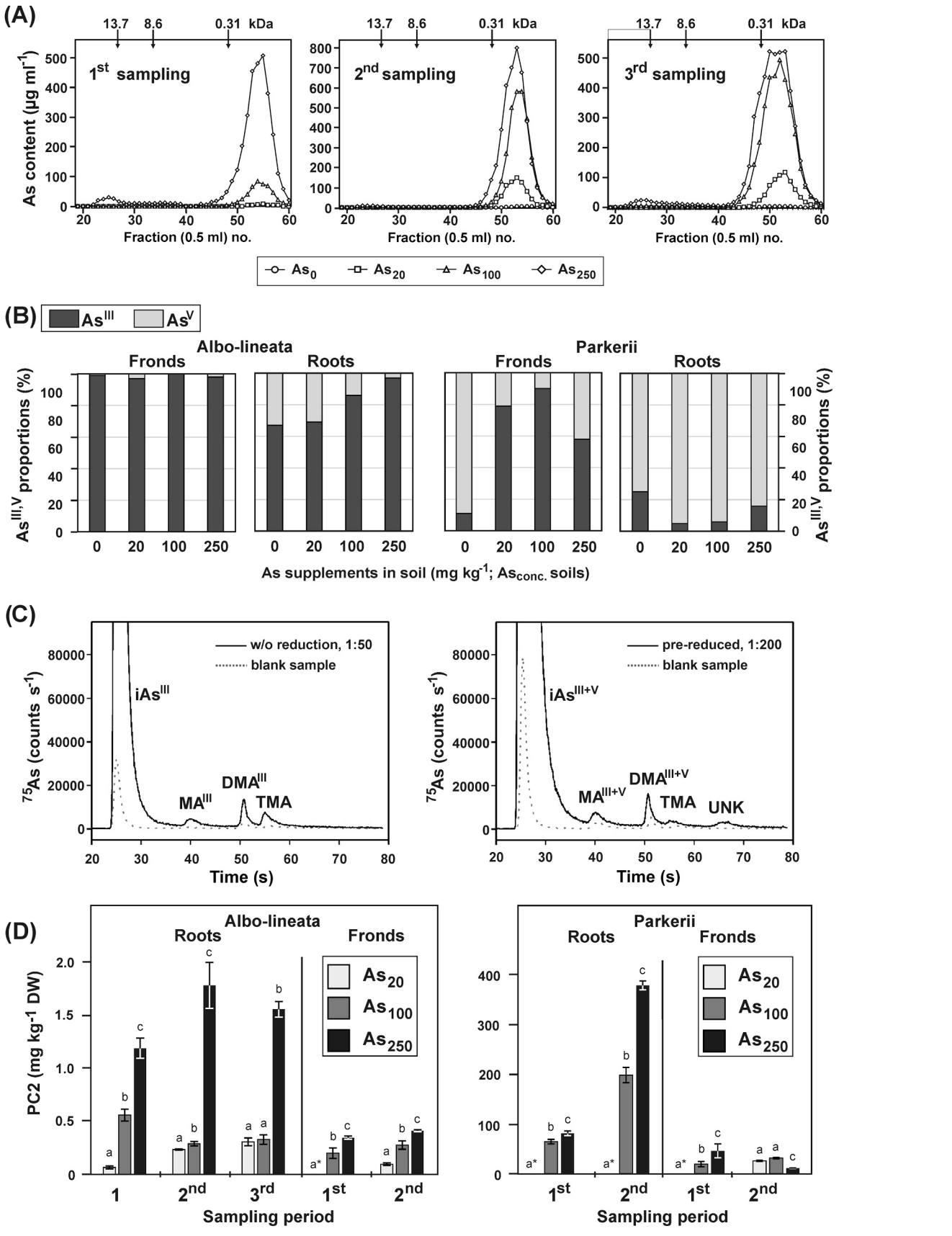

(caption on next page)

Fig. 2. Analyses of As speciation and PCs in As-exposed *P. cretica*. (A) Size exclusion chromatography (SEC) of cell-free extracts from the fronds of As-exposed Albo-lineata. The elution maxima of the molecular mass standards are indicated by arrows. The As content of individual fractions was measured by ICP-OES. (B) Percentage of iAs^{III} and iAs^{V} assessed trough HG-CT-ICP-MS analysis in fronds and roots after 90 d of growth in indicated soils. Plotted were mean values of two replicate measurements with a span of less than 10%. (C) Example spectra obtained for roots of Parkerii (90 d of growth in As_{20} soil) in which individual As species seen with the extracts without pre-reduction (*left panel*; dilution factor 50) and pre-reduced extracts (*right panel*; dilution factor 200) are indicated (UNK, unknown compound). (D) Concentrations of PC2 in the extracts from frond and root tissues assessed by RP-HPLC of molecules labeled with 7-fluorobenzofurazan-4-sulfonic acid (SBD-F). Displayed are samplings and tissues in which the PC2 levels exceeded the limit of quantification of 5 μg kg^{-1} dwt; different letters above the bars indicate significant differences ($n = 3$; $p < 0.05$, Welch's test followed by Games–Howell test) of data plotted for a particular treatment.

Table 2
Concentrations (per dry weight) of organoarsenicals in roots of *P. cretica* cv. Parkerii analyzed after 90 days of vegetation in indicated soils. Data are mean values of two replicate measurements with a span of less than 10%.

Soil	Organoarsenicals as As (μg kg^{-1})					
	MA^{III}	MA^{III+V}	DMA^{III}	DMA^{III+V}	TMA	UNK
As_0	n.d.[a]	0.35	n.d.[a]	0.47	n.d.[a]	2.05
As_{20}	0.49	1.29	0.95	4.29	0.63	2.30
As_{100}	6.98	12.0	n.d.[a]	n.d.[a]	n.d.[a]	16.8
As_{250}	10.2	16.7	3.18	n.d.[a]	4.26	21.5

[a] Below limit of detection in diluted samples.

PvHAC1/2 (Liu et al., 2020) proteins. The ability of this variety to accumulate, translocate, and tolerate high amounts of As further pointed to arsenite transporter, ACR3 protein, with potential roles in iAs^{III} efflux to vacuoles or out of the cells, for safe intracellular sequestration or translocation, respectively. Taking the advantage of the known sequences of the *P. vittata* Pv*ACR2* and Pv*ACR3* mRNA sequences, a homology cloning approach was used to amplify the genomic fragments and coding cDNA sequences of the corresponding Pc*ACR*s from Albo-lineata. The mRNA-to-genomic sequence alignments revealed the presence of two introns in Pc*ACR2*, which are 144 bp long (in codon 30) and 133 bp long (between codons 77 and 78), and a single, 602-bp intron (in codon 34) in Pc*ACR3*; all introns were flanked by canonical |GT-AG| junctions.

The predicted 134-amino acid (AA) PcACR2 shared 88% identity with PvACR2 of *P. vittata* (Ellis et al., 2006) and a hypothetical ACR2 deduced from the *Pteris ensiformis* transcriptome sequence ERR2040935 (Leebens-Mack et al., 2019). Nearly 40% identity was observed with AtACR2 (*syn.* AtSTR5 or AtCDC25) and OsACR2.1 or OsACR2.2 characterized as arsenate reductases in *Arabidopsis thaliana* (Dhankher et al., 2006) and *Oryza sativa* (Duan et al., 2007), respectively, which all by homology belong to the sulfurtransferase (STR)/rhodanase family (Selles et al., 2019). As documented in Fig. 3A, deduced PcACR2 contains the features described in other plant ACR2 proteins. These include the rhodanase homology domain mapping between residues 20 and 125 (PcACR2 numbering) and containing an 8-AA-long sequence motif with catalytic, arsenate-binding Cys^{73} (Most and Papenbrock, 2015), and conserved His^{40}, Cys^{124}, Cys^{126}, and Cys^{131}, which are in AtACR2 known to form a binding site for a structural Zn ion (Landrieu et al., 2004). It is worth noting that Cys^{73} is in PcACR2, like in PvACR2, contained in the H^{72}CGKSQH**S**^{79} sequence, which does not conform to the $HC(X)_5$**R** consensus (X represents any AA; bold letters indicate the difference that lies in Arg instead of Ser^{79}) conserved in other STR/rhodanase proteins and believed to be prerequisite for reductase and phosphatase activity (Selles et al., 2019). Interestingly, the single point mutation that produces Ser^{79} both in PcACR2 and PvACR2 (which possesses reductase but not phosphatase, activity; Ellis et al., 2006) is absent from the hypothetical PeACR2 of *P. ensiformis* (Fig. 3A), which, unlike *P. vittata* and *P. cretica*, is not considered As-hyperaccumulating fern (Meharg, 2003; Singh et al., 2006; Zhang et al., 2017 and references therein). The R→S mutation near catalytic Cys^{73} lies proximal to a potentially mutation-susceptible exon-intron junction. The local synteny with sequences encoding the $HC(X)_5$R motif split to six codon and two codon parts in Pc*ACR2* and Pv*ACR2* genes (HCGKSQ^{76}-intron 2-H^{78}S) can be seen also in *ACR2* genes of *A. thaliana* and *O. sativa* (not shown). However, the possibility that R → S has a relevance to hyperaccumulating phenotype remains speculative, also because the rhizome- and frond-expressed PvHAC1 and PvHAC2, respectively, conserve R in their predicted active site motif C-X_4-R (Li et al., 2020).

As shown in Fig. 3B, the 379-AA protein predicted from Pc*ACR3* shared a high degree of identity to arsenite ACR3 transporters characterized in *P. vittata* (Chen et al., 2017; Indriolo et al., 2010); it appeared nearly identical to the vacuolar PvACR3 (92% identity) and shared 71% identity with PvACR3;1. Moreover, it shared a substantial identity (42%) with the bacterial CgAcr3 from *Corynebacterium glutamicum*. Like the aforementioned proteins, PcACR3 has 10 predicted transmembrane domains (TMDs) with N and C termini localized to the cytoplasm. The regions showing the highest proportion of residues conserved in all aligned ACR3s involved TMD4 and TMD9 with their Cys^{160} and Glu^{331}, respectively. The corresponding residues were shown indispensable for the transport function of CgAcr3 mediated through iAs^{III}-H^{+} antiport (Villadangos et al., 2012).

The 650-bp genomic sequence upstream of Pc*ACR3*, obtained from the genome walking experiment, was used to analyze the promoter region for potential As-related, *cis*-acting transcription factor (TF) binding sites. The screening against JASPAR CORE Plant database returned putative target sites for TFs from the Dof family, which have been found in *Arabidopsis thaliana* and other plants involved in abiotic stress tolerance (Cheng et al., 2018; Corrales et al., 2017) and for PHL2 acting as a key component under phosphate starvation (Sun et al., 2016).

3.4. As tolerance in yeasts expressing PcACR2 and PcACR3

To obtain information about the capability of PcACRs to protect the cells from As toxicity, the coding sequences of Pc*ACR2* and Pc*ACR3* genes were inserted into the vector p426GPD for the constitutive expression in the As-sensitive *S. cerevisiae* BY4741 strains: *acr2*Δ in which the arsenate reductase was inactivated, and *acr3*Δ lacking the plasma membrane exporter. As documented in Fig. 4, both Pc*ACR2* and Pc*ACR3* conferred increased As tolerance to the respective yeast mutants. In the plate assays on As-spiked solid SD medium, the expression of Pc*ACR2* complemented the As sensitivity of *acr2*Δ mutant in the presence of 15 mM arsenate. While 2 mM arsenite fully inhibited growth of parental BY4741 yeast, this As concentration was not fully detrimental to the growth of Pc*ACR3*-expressing *acr3*Δ cells (Fig. 4A). The protective effect of Pc*ACR*s against As toxicity was also evident when dose-dependent inhibitory effect of As was monitored in liquid SD medium supplemented with increasing concentrations of As to determine the concentrations impairing the growth of the yeasts by 50% (IC_{50As}) (Fig. 4B). The IC_{50AsV} of the Pc*ACR2*-expressing mutant was 12 times higher than that of mere *acr2*Δ cells and essentially the same as the IC_{50AsV} of the parental BY4741 strain. The expression of Pc*ACR3* increased the $IC_{50AsIII}$ of *acr3*Δ yeast more than 18 times than p426GPD-only transformed *acr3*Δ, and, moreover, 2.2 times compared to the parental BY4741 strain.

To obtain additional information about Pc*ACR3*-associated As tolerance phenotype, the accumulation of As was investigated in the *acr3*Δ yeasts incubated for 1 h in SD medium supplemented with arsenite and arsenate (expected to be reduced in vivo) as potential substrates for PcACR3-mediated transport. It was also reasonable to assume that if the functional PcACR3 exported As out of the cell or funneled it into the vacuoles in the *acr3*Δ strain, its function in vivo could be that of a

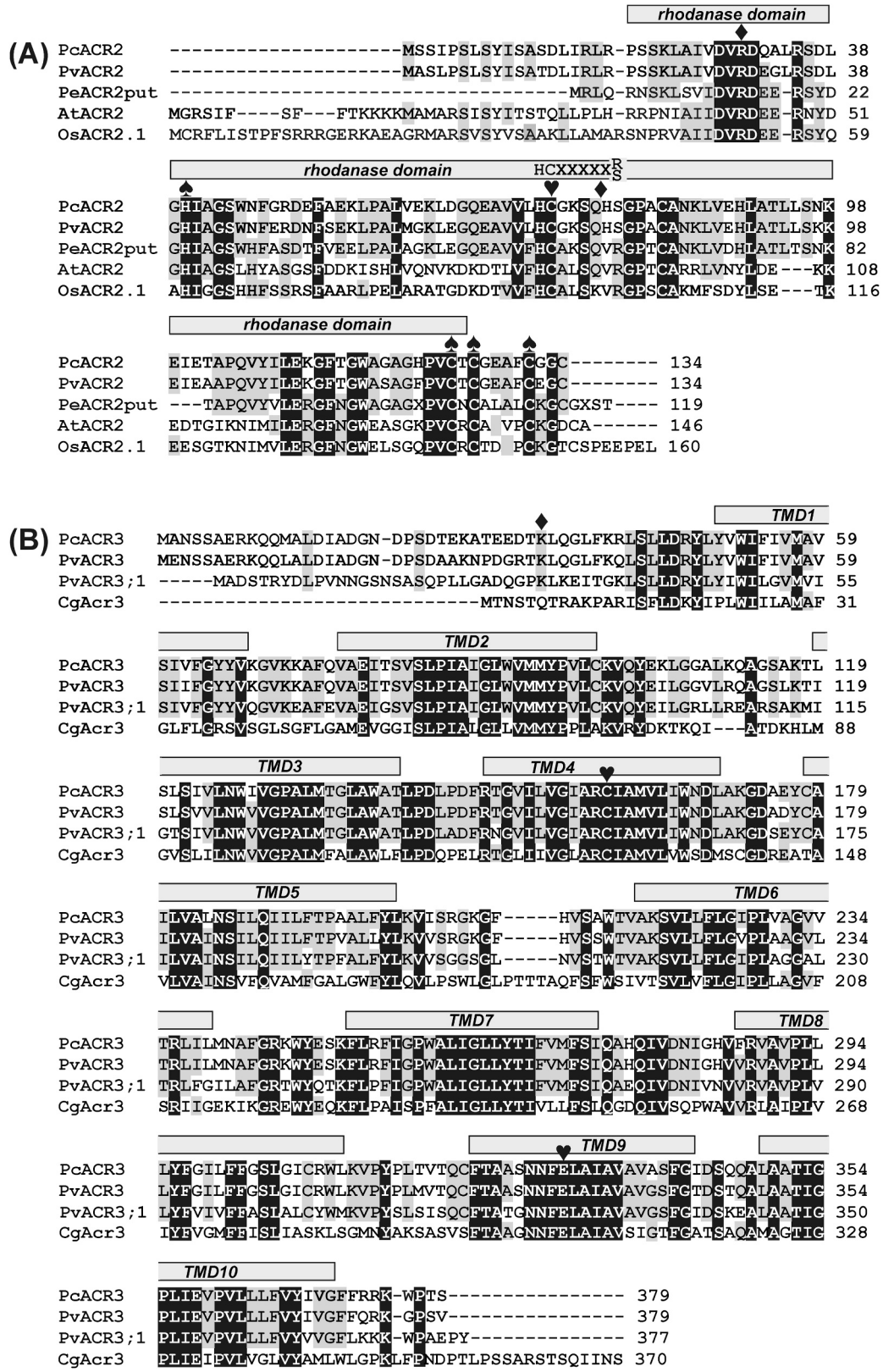

Fig. 3. Alignment of predicted PcACR2 (A) and PcACR3 (B) proteins with functionally characterized homologs from *P. vittata* (Pv), *A. thaliana* (At), *O. sativa* (Os), *C. glutamicum* (Cg) and putative arsenate reductase from *P. ensiformis* (Pe). Conserved amino acid residues are boxed (those identical in all sequences are marked with black background). Indicated are the positions of predicted rhodanase domain with $HC(X)_5R/S$ motif, transmembrane domains (TMD), known essential residues (hearts), Zn binding residues (spades), and the interruptions within corresponding genes by introns (diamonds). The GenBank accession numbers are as follows: *Pteris vittata* PvACR2, ABC26900; PvACR3, ADP20983; PvACR3;1, ASV64940; *Pteris ensiformis*, ERR2040935; *Arabidopsis thaliana* AtACR2, NP_568119; *Oryza sativa* OsACR2.1, XP_015612765; *Corynebacterium glutamicum* CgAcr3, WP_080724106; PcACR2, MW027137; PcACR3, MW027138.

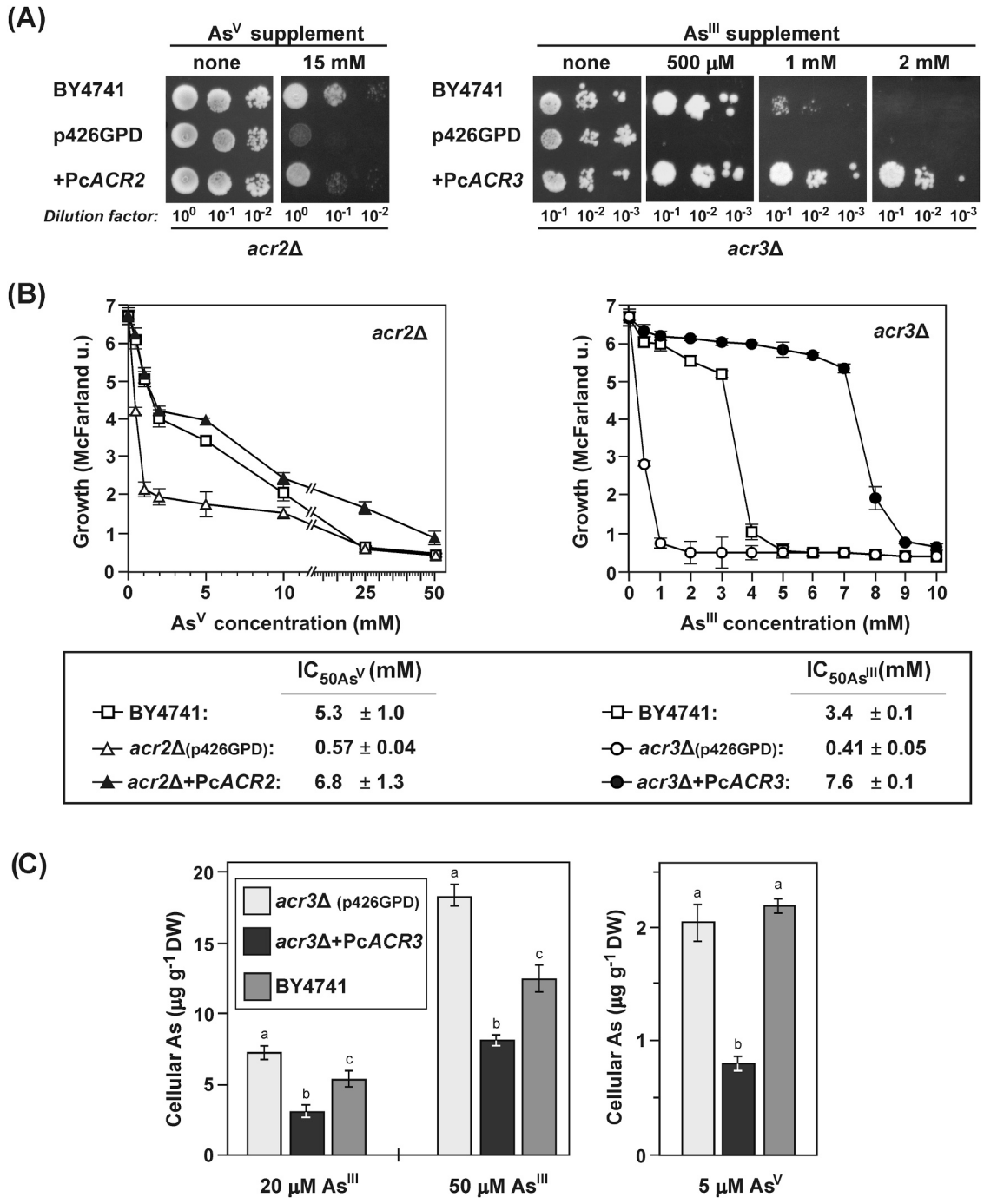

Fig. 4. Functional expression of Pc*ACR2* and Pc*ACR3* in As-sensitive *Saccharomyces cerevisiae* strains. (A) Indicated mutant strains were transformed with an empty p426GPD vector or with the same expression vector inserted with the coding sequences of individual Pc*ACR*s. Diluted transformant cultures were spotted on SD medium with or without As supplement as indicated. Displayed is also parental As-tolerant strain BY4741. (B) Dose-dependent growth inhibition of yeasts (same as panel A) in liquid media. Individual transformants were grown in SD media with different concentrations of As and the turbidity of the culture was measured after 48 h. The As concentrations resulting in 50% reduction in the culture turbidity (IC_{50As}) calculated by fitting the data to the sigmoidal inhibition curve are indicated. Values are the mean of three independent biological replicates ± standard deviation. (C) Accumulation of As in *acr3*Δ strain expressing Pc*ACR3*. The As content was measured in the control p426GPD-transformed and Pc*ACR3*-expressing *acr3*Δ cells and in BY4741 yeasts following 1 h incubation in SD medium supplemented with 20 and 50 μM arsenite or 5 μM arsenate. The values represent the average of at least three biological replicates ± standard deviation of the mean (the values proved significantly different from each other at $p < 0.05$ level as determined by Welch's test followed by Games–Howell test).

plasma membrane transporter, reducing intracellular As, or a vacuolar transporter, allowing safe cellular (over)accumulation of As, respectively. As shown in Fig. 4C, the expression of Pc*ACR3* significantly reduced the concentrations of As in *acr3*Δ yeasts exposed to 20 μM or 50 μM arsenite (more than 2.3 times) and 5 μM arsenate (2.6 times). Congruent with the markedly higher As tolerance in the Pc*ACR3*-expressing *acr3*Δ mutant compared to BY4741 cells (Fig. 4A and B), the ability of parental BY4741 strain with its innate ScACR3 plasma membrane exporter (Wysocki et al., 1997) to eliminate arsenite from the cells under the same conditions was less pronounced (Fig. 4C). Taken together, these data convincingly show that PcACR3 is a genuine As transporter, which in model yeasts localized, like ScACR3, to the plasma

membrane for As efflux. Noteworthy and like in the yeasts, PvACR3 localized to the plasma membrane when expressed in *A. thaliana*, apparently supporting the root-to-shoot translocation by loading the xylem sap with the root As (Wang et al., 2018; Chen et al., 2013). It must be stressed, however, that PvACR3 clearly localized to the vacuoles, but not the plasma membrane, in *P. vittata* (Indriolo et al., 2010), supporting the deposition of As in vacuoles in aboveground parts of the fern. Considering high degree of sequence homology with PcACR3 and that mislocalization of heterologous membrane proteins in yeasts may occur, as it was the case also with PvACR3;1 (Chen et al., 2017), it appears reasonable to expect PcACR3 localizing to vacuole tonoplast, being largely responsible for vacuolar sequestration and thus detoxification of As hyperaccumulated in Albo-lineata fronds. This observation would also be in congruence with the high contents of As in Albo-lineata, as discussed previously.

3.5. As-dependent accumulation of PcACR2 and PcACR3 transcripts in Albo-lineata

Considering that higher concentrations of As accumulated in Albo-lineata pose a higher demand on the expression of Pc*ACR2* and Pc*ACR3* genes, their transcription rates were analyzed by using qRT-PCR, measuring corresponding mRNA levels in the fronds of plants exposed to As for 90 d. Compared to the As_0 plants, used as a reference, the fronds of plants grown in soils supplemented with additional As showed significantly increased levels of Pc*ACR* transcripts with the maximum accumulation of Pc*ACR2* and Pc*ACR3* mRNAs (more than 6.5- and 45-fold increase, respectively) observed with As_{100} plants (Fig. 5). This is in a good alignment with the observed translocation factor calculated for this sample, especially when considering a markedly raised accumulation capacity between the 1st and 2nd sampling on As_{100} (Table 1). The observed substantial increase in Pc*ACR3* transcripts in As-exposed Albo-lineata further strengthens the notion that PcACR3 transporter is involved in the detoxification of iAs^{III} through its subcellular compartmentalization in the fronds. Considering that the As-responsive increase in ACR2 arsenate reductase activity has been in *P. vittata* observed in roots, whilst it was undetectable in fronds (Duan et al., 2005), it would be interesting to see whether and to what extent the transcription rates of Pc*ACR2* exceed those in fronds. Regrettably, our attempts to assess the transcription in roots failed; the RNA quality was low, likely due to the deterioration of root RNA during sampling and storage. Furthermore, high and apparently constitutive levels of Pv*HAC2* accompanied with low relative expression of Pv*ACR2* not responding to As exposures in *P. vittata* fronds (Li et al., 2020) rise a hypothesis, whether or not *P. cretica* has a full inventory of As-handling determinants akin to *P. vittata*.

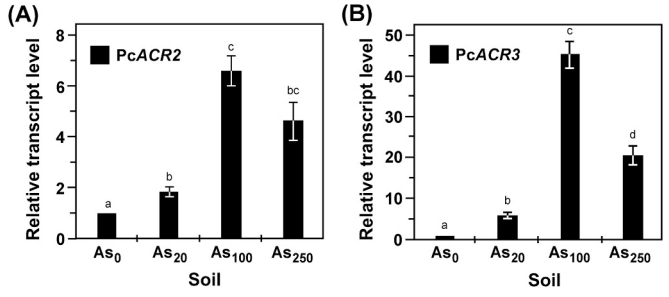

Fig. 5. Expression of Pc*ACR* genes in *P. cretica* cv. Albo-lineata. The levels of Pc*ACR2* (A) and Pc*ACR3* (B) transcripts were measured by qRT-PCR in the fronds of 3 plants grown in the indicated soils for 90 d. The Pc*ACR* mRNA levels are referred to the plants grown in As_0 soil (value of 1) and for each condition was the value plotted as an average relative mRNA level ± standard deviation of the mean of three biological replicates (the values proved significantly different from each other at $p < 0.05$ level as determined by Welch's test followed by Games–Howell test).

4. Conclusions

The last two decades brought a substantial body of information about the natural capacity of certain ferns, particularly of *P. vittata*, to hyperaccumulate As, and about the underlying cell and plant biology of As as well. The research interest into the hyperaccumulation phenomenon, related biology, and the potential for the phytoextraction of As from damaged soils, was more recently dedicated also to several varieties of *P. cretica* (Claveria et al., 2019; Eze and Harvey, 2018; Jeong et al., 2014, 2015; Rahman et al., 2018; Zhang et al., 2017), including Albo-lineata and Parkerii (Pavlíková et al., 2017, 2020; Zemanová et al., 2019, 2020). To the best of our knowledge, the Pc*ACR2* and Pc*ACR3* described here are the second genes encoding arsenate reductase ACR2 and arsenite transporter ACR3 characterized so far in *Pteris* spp. The characteristic sequence features of the encoded proteins, significant protection against iAs toxicity conferred to yeasts by corresponding cDNAs, and As-responsiveness of the Pc*ACR* genes *in planta* provide the evidence that PcACRs proteins can beregarded as determinants involved in hyperaccumulation of As in Albo-lineata. Besides the first role we propose for PcACR2, i.e. reducing As^V in roots, the abundance of PcACR2 transcripts in fronds indicates an additional role in the reduction of As^V in fronds, that may have eventually escaped roots for translocation and/or that might have arisen in frond cells from re-oxidation of stored As^{III} (Tu et al., 2003; Wan et al., 2018; Zhang et al., 2017). Whether or not *P. cretica* cultivars encode other arsenate reductases in addition to PcACR2, as it is the case in *P. vittata* with its PvACR2, rhizome PvHAC1 and frond PvHAC2 proteins (Li et al., 2020) and the sporophyte may benefit from complementation by bacterial-like pathway (involving in *P. vittata* sporophytes PvGAPC1, PvOCT4, and PvGSTF1; Cai et al., 2019), and what would be their interplay in As^V reduction in Albo-lineata remains to be investigated.

Considering the high degree of sequence homology with PvACR3s and that mislocalization of heterologous membrane proteins in yeasts may occur, as it was also the case with PvACR3;1 (Chen et al., 2017), it appears reasonable to expect PcACR3 localizing to tonoplast, and thus being largely responsible for vacuolar sequestration and detoxification of iAs hyperaccumulated in Albo-lineata fronds.

The As uptake and tolerance data presented in this study further support our notion that Albo-lineata represents genuine As-hyperaccumulating cultivar, whilst Parkerii, reported previously as hyperaccumulator (Meharg, 2003), is to be considered a non-hyperaccumulating one (Pavlíková et al., 2020; Zemanová et al., 2020). Our data revealing very low PC and OAs levels in *P. cretica*, features associated with Pc*ACR*s, and lessons taken from studies in *P. vittata* lead us to the conclusion that $iAs^{III/V}$ are central in the biology of As in both *P. cretica* cultivars examined in this study.

Author contributions

PK, MPa and DP conceived the presented idea and planned the experiments. MPo carried out most of the experimental work in biochemical and molecular analyses. VP and MPa prepared plant material and conducted As analyses. TM analyzed (organo)arsenicals. AK and JS conducted the As uptake assay in yeasts. AK performed the statistic. JS and TL jointly contributed to the design of molecular works and the bioinformatic analyses. PK ensured the scientific issue was appropriately investigated and together with TL was responsible for the final interpretation of the results, and writing the manuscript. All authors provided critical data analysis and feedback, helped shape the research and manuscript, and approved the final version of the manuscript.

Declaration of Competing Interest

All the authors declare that they have no conflicts of interest with regards to this work and that all of the sources of funding for this work are acknowledged.

Acknowledgments

We are very thankful to Hana Zámečníková for an excellent technical support in ICP-OES measurements. This work has been supported by the Czech Science Foundation (Grant No. 17-10591S). The support from Ministry of Education, Youth and Sports of the Czech Republic (ERDF Project CZ.02.1.01/0.0/0.0/16_019/0000845) to Czech University of Life Science and the institutional support (RVO: 68081715) to the Institute of Analytical Chemistry of the Czech Academy of Sciences the Czech are also gratefully acknowledged.

References

Abid, R., Manzoor, M., De Oliveira, L.M., da Silva, E., Rathinasabapathi, B., Rensing, C., Mahmood, S., Liu, X., Ma, L.Q., 2019. Interactive effects of As, Cd and Zn on their uptake and oxidative stress in As-hyperaccumulator *Pteris vittata*. Environ. Pollut. 248, 756–762. https://doi.org/10.1016/j.envpol.2019.02.054.

Abou-Shanab, R.A.I., Mathai, P.P., Santelli, C., Sadowsky, M.J., 2020. Indigenous soil bacteria and the hyperaccumulator *Pteris vittata* mediate phytoremediation of soil contaminated with arsenic species. Ecotoxicol. Environ. Saf. 195, 110458 https://doi.org/10.1016/j.ecoenv.2020.110458.

Allevato, E., Stazi, S.R., Marabottini, R., D'Annibale, A., 2019. Mechanisms of arsenic assimilation by plants and countermeasures to attenuate its accumulation in crops other than rice. Ecotoxicol. Environ. Saf. 185, 109701 https://doi.org/10.1016/j.ecoenv.2019.109701.

Ashkenazy, H., Abadi, S., Martz, E., Chay, O., Mayrose, I., Pupko, T., Ben-Tal, N., 2016. ConSurf 2016: an improved methodology to estimate and visualize evolutionary conservation in macromolecules. Nucleic Acids Res. 44, 344–350. https://doi.org/10.1093/nar/gkw408.

Beneš, V., Leonhardt, T., Kaňa, A., Sácký, J., Kotrba, P., 2019. Heterologous expression of Zn-binding peptide RaZBP1 from *Russula bresadolae* does not overcome Zn and Cd detoxification mechanisms in *Hebeloma mesophaeum*. Folia Microbiol. 64, 835–844. https://doi.org/10.1007/s12223-019-00696-1.

Braeuer, S., Goessler, W., Kameník, J., Konvalinková, T., Žigová, A., Borovička, J., 2018. Arsenic hyperaccumulation and speciation in the edible ink stain bolete (*Cyanoboletus pulverulentus*). Food Chem. 242, 225–231. https://doi.org/10.1016/j.foodchem.2017.09.038.

Cai, C., Lanman, N.A., Withers, K.A., DeLeon, A.M., Wu, Q., Gribskov, M., Salt, D.E., Banks, J.A., 2019. Three genes define a bacterial-like arsenic tolerance mechanism in the arsenic hyperaccumulating fern *Pteris vittata*. Curr. Biol. 29, 1625–1633. https://doi.org/10.1016/j.cub.2019.04.029.

Cao, Y., Sun, D., Chen, J.-X., Mei, H., Xu, G., Chen, Y., Ma, L.Q., 2018. Phosphate transporter PvPht1;2 enhances phosphorus accumulation and plant growth without impacting arsenic uptake in plants. Environ. Sci. Technol. 52, 3975–3981. https://doi.org/10.1021/acs.est.7b06674.

Chen, Y., Xu, W., Shen, H., Yan, H., Xu, W., He, Z., Ma, M., 2013. Engineering arsenic tolerance and hyperaccumulation in plants for phytoremediation by a PvACR3 transgenic approach. Environ. Sci. Technol. 47, 9355–9362. https://doi.org/10.1021/es4012096.

Chen, Y., Fu, J.-W., Han, Y.-H., Rathinasabapathi, B., Ma, L.Q., 2016. High As exposure induced substantial arsenite efflux in As-hyperaccumulator *Pteris vittata*. Chemosphere 144, 2189–2194. https://doi.org/10.1016/j.chemosphere.2015.11.001.

Chen, Y., Hua, C.-Y., Jia, M.-R., Fu, J.-W., Liu, X., Han, Y.-H., Liu, Y., Rathinasabapathi, B., Cao, Y., Ma, L.Q., 2017. Heterologous expression of *Pteris vittata* arsenite antiporter PvACR3;1 reduces arsenic accumulation in plant shoots. Environ. Sci. Technol. 51, 10387–10395. https://doi.org/10.1021/acs.est.7b03369.

Cheng, Z., Hou, D., Liu, J., Li, X., Xie, L., Ma, Y., Gao, J., 2018. Characterization of moso bamboo (*Phyllostachys edulis*) Dof transcription factors in floral development and abiotic stress responses. Genome 61, 151–156. https://doi.org/10.1139/gen-2017-0189.

Claveria, R.J.R., Perez, T.R., Apuan, M.J.B., Apuan, D.A., Perez, R.E.C., 2019. Pteris melanocaulon Fée is an As hyperaccumulator. Chemosphere 236, 124380. https://doi.org/10.1016/j.chemosphere.2019.124380.

Corrales, A.R., Carrillo, L., Lasierra, P., Nebauer, S.G., Dominguez-Figueroa, J., Renau-Morata, B., Pollmann, S., Granell, A., Molina, R.V., Vicente-Carbajosa, J., Medina, J., 2017. Multifaceted role of cycling DOF factor 3 (CDF3) in the regulation of flowering time and abiotic stress responses in *Arabidopsis*. Plant Cell Environ. 40, 748–764. https://doi.org/10.1111/pce.12894.

Cui, J., Jing, Ch., 2019. A review of arsenic interfacial geochemistry in groundwater and the role of organic matter. Ecotoxicol. Environ. Saf. 183, 109550 https://doi.org/10.1016/j.ecoenv.2019.109550.

Currier, J.M., Svoboda, M., de Moraes, D.P., Matoušek, T., Dědina, J., Stýblo, M., 2011. Direct analysis of methylated trivalent arsenicals in mouse liver by hydride generation-cryotrapping-atomic absorption spectrometry. Chem. Res. Toxicol. 24, 478–480. https://doi.org/10.1021/tx200060c.

da Silva, E.B., Lessl, J.T., Wilkie, A.C., Liu, X., Liu, Y.G., Ma, L.N.Q., 2018. Arsenic removal by As-hyperaccumulator *Pteris vittata* from two contaminated soils: A 5-year study. Chemosphere 206, 736–741. https://doi.org/10.1016/j.chemosphere.2018.05.055.

Dhankher, O.P., Rosen, B.P., McKinney, E.C., Meagher, R.B., 2006. Hyperaccumulation of arsenic in the shoots of *Arabidopsis* silenced for arsenate reductase (ACR2). Proc. Natl. Acad. Sci. USA 103, 5413–5418. https://doi.org/10.1073/pnas.0509770102.

Di, X.R., Beesley, L., Zhang, Z.L., Zhi, S.L., Jia, Y., Ding, Y.Z., 2019. Microbial arsenic methylation in soil and uptake and metabolism of methylated arsenic in plants: a review. IJERPH 16, 5012. https://doi.org/10.3390/ijerph16245012.

DiTusa, S.F., Fontenot, E.B., Wallace, R.W., Silvers, M.A., Steele, T.N., Elnagar, A.H., Dearman, K.M., Smith, A.P., 2016. A member of the phosphate transporter 1 (Pht1) family from the arsenic-hyperaccumulating fern *Pteris vittata* is a high-affinity arsenate transporter. New Phytol. 206, 762–772. https://doi.org/10.1111/nph.13472.

Duan, G.L., Zhu, Y.G., Tong, Y.P., Cai, C., Kneer, R., 2005. Characterization of arsenate reductase in the extract of roots and fronds of Chinese brake fern, an arsenic hyperaccumulator. Plant Physiol. 138, 461–469. https://doi.org/10.1104/pp.104.057422.

Duan, G.L., Zhou, Y., Tong, Y.P., Mukhopadhyay, R., Rosen, B.P., Zhu, Y.G., 2007. A CDC25 homologue from rice functions as an arsenate reductase. New Phytol. 2007, 311–321. https://doi.org/10.1111/j.1469-8137.2007.02009.x.

Ellis, D.R., Gumaelius, L., Indriolo, E., Pickering, I.J., Banks, J.A., Salt, D.E., 2006. A novel arsenate reductase from the arsenic hyperaccumulating fern *Pteris vittata*. Plant Physiol. 141, 1544–1554. https://doi.org/10.1104/pp.106.084079.

Eze, V.C., Harvey, A.P., 2018. Extractive recovery and valorisation of arsenic from contaminated soil through phytoremediation using *Pteris cretica*. Chemosphere 208, 484–492. https://doi.org/10.1016/j.chemosphere.2018.06.027.

Feng, H., Li, X., Chen, Y., Xu, G., Ma, L.Q., 2021. Expressing phosphate transporter PvPht2;1 enhances P transport to the chloroplasts and increase arsenic tolerance in *Arabidopsis thaliana*. Environ. Sci. Technol. 55, 2276–2284. https://doi.org/10.1021/acs.est.0c03316.

Fu, J.W., Liu, X., Han, Y.H., Mei, H.Y., Cao, Y., de Oliveira, L.M., Liu, Y.G., Rathinasabapathi, B., Chen, Y.S., Ma, L.Q., 2017. Arsenic-hyperaccumulator *Pteris vittata* efficiently solubilized phosphate rock to sustain plant growth and As uptake. J. Hazard. Mater. 330, 68–75. https://doi.org/10.1016/j.jhazmat.2017.01.049.

Han, Y.H., Liu, X., Rathinasabapathi, B., Li, H.B., Chen, Y.S., Ma, L.Q., 2017. Mechanisms of efficient As solubilization in soils and As accumulation by As-hyperaccumulator *Pteris vittata*. Environ. Pollut. 227, 569–577. https://doi.org/10.1016/j.envpol.2017.05.001.

He, Z.Y., Yan, H.L., Chen, Y.S., Shen, H.L., Xu, W.X., Zhang, H.Y., Shi, L., Zhu, Y.G., Ma, M., 2016. An aquaporin PvTIP4;1 from *Pteris vittata* may mediate arsenite uptake. New Phytol. 209, 746–761. https://doi.org/10.1111/nph.13637.

Hložková, K., Matěnová, M., Žáčková, P., Strnad, H., Hršelová, H., Hroudová, M., Kotrba, P., 2016. Characterization of three distinct metallothionein genes of the Ag-hyperaccumulating ectomycorrhizal fungus *Amanita strobiliformis*. Fungal Biol. 120, 358–369. https://doi.org/10.1016/j.funbio.2015.11.007.

Indriolo, E., Na, G., Ellis, D., Salt, D.E., Banks, J.A., 2010. A vacuolar arsenite transporter necessary for arsenic tolerance in the arsenic hyperaccumulating fern *Pteris vittata* is missing in flowering plants. Plant Cell 22, 2045–2057. https://doi.org/10.1105/tpc.109.069773.

Jeong, S., Moon, H.S., Nam, K., 2014. Enhanced uptake and translocation of arsenic in Cretan brake fern (*Pteris cretica* L.) through siderophorearsenic complex formation with an aid of rhizospheric bacterial activity. J. Hazard. Mater. 280, 536–543. https://doi.org/10.1016/j.jhazmat.2014.08.057.

Jeong, S., Moon, H.S., Nam, K., 2015. Increased ecological risk due to the hyperaccumulation of As in *Pteris cretica* during the phytoremediation of an As-contaminated site. Chemosphere 122, 1–7. https://doi.org/10.1016/j.chemosphere.2014.10.003.

Käll, L., Krogh, A., Sonnhammer, E.L.L., 2007. Advantages of combined transmembrane topology and signal peptide prediction-the Phobius web server. Nucleic Acids Res. 35, 429–432. https://doi.org/10.1093/nar/gkm256.

Landrieu, I., da Costa, M., De Veylder, L., Dewitte, F., Vandepoele, K., Hassan, S., Wieruszeski, J.M., Faure, J.D., Van Montagu, M., Inzé, D., Lippens, G., 2004. A small CDC25 dual-specificity tyrosine-phosphatase isoform in *Arabidopsis thaliana*. Proc. Natl. Acad. Sci. USA 101, 13380–13385. https://doi.org/10.1073/pnas.0405248101.

Larsen, E.H., Hansen, M., Gössler, W., 1998. Speciation and health risk considerations of arsenic in the edible mushroom *Laccaria Amethystina* collected from contaminated and uncontaminated locations. Appl. Organomet. Chem. 12, 285–291, 10.1002/(SICI)1099-0739(199804)12:4<285::AID-AOC706>3.3.CO;2-R.

Lebow, S., Foster, D., Lebow, P., 2004. Rate of CCA leaching from commercially treated decking. For. Prod. J. 54, 81–88.

Leebens-Mack, J.H., Barker, M.S., Carpenter, E.J., et al., 2019. One thousand plant transcriptomes and the phylogenomics of green plants. Nature 574, 679–685. https://doi.org/10.1038/s41586-019-1693-2.

Li, N., Wang, J., Song, W.-Y., 2016. Arsenic uptake and translocation in plants. Plant Cell Physiol. 57, 4–13. https://doi.org/10.1093/pcp/pcv143.

Li, X., Sun, D., Feng, H., Chen, J., Li, H., Cao, Y., Ma, L.Q., 2020. Efficient arsenate reduction in As-hyperaccumulator Pteris vittata are mediated by novel arsenate reductases PvHAC1 and PvHAC2. J. Hazard. Mater. 399, 122895 https://doi.org/10.1016/j.jhazmat.2020.122895.

Liu, W.J., Wood, B.A., Raab, A., McGrath, S.P., Zhao, F.-J., Feldmann, J., 2010. Complexation of arsenite with phytochelatins reduces arsenite efflux and translocation from roots to shoots in *Arabidopsis*. Plant Physiol. 152, 2211–2221. https://doi.org/10.1104/pp.109.150862.

Liu, X., Feng, H.Y., Fu, J.W., Sun, D., Cao, Y., Chen, Y.S., Xiang, P., Liu, Y.G., Ma, L.Q., 2018. Phytate promoted arsenic uptake and growth in arsenic-hyperaccumulator *Pteris vittata* by upregulating phosphorus transporters. Environ. Pollut. 241, 240–246. https://doi.org/10.1016/j.envpol.2018.05.054.

Ma, L.Q., Komar, K.M., Tu, C., Zhang, W.H., Cai, Y., Kennelley, E.D., 2001. A fern that hyperaccumulates arsenic. Nature 409, 579. https://doi.org/10.1038/35078151.

Madejón, P., Dominguez, M.T., Madejon, E., Cabrera, F., Maranon, T., Murillo, J.M., 2018. Soil-plant relationships and contamination by trace elements: a review of twenty years of experimentation and monitoring after the Aznalcollar (SW Spain) mine accident. Sci. Total Environ. 625, 50–63. https://doi.org/10.1016/j.scitotenv.2017.12.277.

Mathelier, A., Zhao, X., Zhang, A.W., Parcy, F., Worsley-Hunt, R., Arenillas, D.J., Buchman, S., Chen, C.Y., Chou, A., Ienasescu, H., Lim, J., Shyr, C., Tan, G., Zhou, M., Lenhard, B., Sandelin, A., Wasserman, W.W., 2013. JASPAR 2014: an extensively expanded and updated open-access database of transcription factor binding profiles. Nucleic Acids Res. 42, 142–147. https://doi.org/10.1093/nar/gkt997.

Matoušek, T., Currier, J.M., Trojánková, N., Saunders, R.J., Ishida, M.C., Gonzalez-Horta, C., Musil, S., Mester, Z., Stýblo, M., Dědina, J., 2013. Selective hydride generation-cryotrapping-ICP-MS for arsenic speciation analysis at picogram levels: analysis of river and sea water reference materials and human bladder epithelial cells. J. Anal. Atom. Spectrom. 28, 1456–1465. https://doi.org/10.1039/c3ja50021g.

Meharg, A.A., 2003. Variation in arsenic accumulation – hyperaccumulation in ferns and their allies. New Phytol. 157, 25–31. https://doi.org/10.1046/j.1469-8137.2003.00541.x.

Most, P., Papenbrock, J., 2015. Possible roles of plant sulfurtransferases in detoxification of cyanide, reactive oxygen species, selected heavy metals and arsenate. Molecules 20, 1410–1423. https://doi.org/10.3390/molecules20011410.

NASEM (National Academies of Sciences, Engineering, and Medicine), 2019. Review of EPA's Updated Problem Formulation and Protocol for the Inorganic Arsenic IRIS Assessment. The National Academies Press, Washington, DC. https://doi.org/10.17226/25558.

Oberoi, S., Devleesschauwer, B., Gibb, H.J., Barchowsky, A., 2019. Global burden of cancer and coronary heart disease resulting from dietary exposure to arsenic, 2015. Environ. Res. 171, 185–192. https://doi.org/10.1016/j.envres.2019.01.025.

Osobová, M., Urban, V., Jedelský, P.L., Borovička, J., Gryndler, M., Ruml, T., Kotrba, P., 2011. Three metallothionein isoforms and sequestration of intracellular silver in hyperaccumulator *Amanita strobiliformis*. New Phytol. 190, 916–926. https://doi.org/10.1111/j.1469-8137.2010.03634.x.

Pavlíková, D., Zemanová, V., Pavlík, M., 2017. The contents of free amino acids and elements in As-hyperaccumulator *Pteris cretica* and non-hyperaccumulator *Pteris straminea* during reversible senescence. Plant Soil Environ. 63, 455–460. https://doi.org/10.17221/606/2017-PSE.

Pavlíková, D., Zemanová, V., Pavlík, M., Dobrev, P.I., Hnilička, F., Motyka, V., 2020. Response of cytokinins and nitrogen metabolism in the fronds of Pteris sp. under arsenic stress. PLoS One 15, e0233055. https://doi.org/10.1371/journal.pone.0233055.

Raab, A., Feldmann, J., Meharg, A.A., 2004. The nature of arsenic-phytochelatin complexes in Holcus lanatus and *Pteris cretica*. Plant Physiol. 134, 1113–1122. https://doi.org/10.1104/pp.103.033506.

Rahman, F., Sugawara, K., Huang, Y., Chien, M.F., Inoue, C., 2018. Arsenic, lead and cadmium removal potential of Pteris multifida from contaminated water and soil. Int. J. Phytoremediat. 20, 1187–1193. https://doi.org/10.1080/15226514.2017.1375896.

Sácký, J., Leonhardt, T., Borovička, J., Gryndler, M., Briksí, A., Kotrba, P., 2014. Intracellular sequestration of zinc, cadmium and silver in *Hebeloma mesophaeum* and characterization of its metallothionein genes. Fungal Genet. Biol. 67, 3–14. https://doi.org/10.1016/j.fgb.2014.03.003.

Selles, B., Moseler, A., Rouhier, N., Couturier, J., 2019. Rhodanese domain-containing sulfurtransferases: multifaceted proteins involved in sulfur trafficking in plants. J. Exp. Bot. 70, 4139–4154. https://doi.org/10.1093/jxb/erz213.

Sigrist, C.J.A., de Castro, E., Cerutti, L., Cuche, B.A., Hulo, N., Bridge, A., Bougueleret, L., Xenarios, I., 2013. New and continuing developments at PROSITE. Nucleic Acids Res. 41, 344–347. https://doi.org/10.1093/nar/gks1067.

Singh, N., Ma, L.Q., 2006. Arsenic speciation, and arsenic and phosphate distribution in arsenic hyperaccumulator *Pteris vittata* L. and non-hyperaccumulator *Pteris ensiformis* L. Environ. Pollut. 141, 238–246. https://doi.org/10.1016/j.envpol.2005.08.050.

Singh, N., Ma, L.Q., Srivastava, M., Rathinasabapathi, B., 2006. Metabolic adaptations to arsenic-induced oxidative stress in *Pteris vittata* L and *Pteris ensiformis* L. Plant Sci. 170, 274–282. https://doi.org/10.1016/j.plantsci.2005.08.013.

Singh, N., Raj, A., Khare, P.B., Tripathi, R.D., Jamil, S., 2010. Arsenic accumulation pattern in 12 Indian ferns and assessing the potential of *Adiantum capillus-veneris*, in comparison to *Pteris vittata*, as arsenic hyperaccumulator. Bioresour. Technol. 101, 8960–8968. https://doi.org/10.1016/j.biortech.2010.06.116.

Sun, D., Feng, H., Li, X., Ai, H., Chen, Y., Xu, G., Rathinasabapathi, B., Cao, Y., Ma, L.Q., 2020. Expression of new *Pteris vittata* phosphate transporter PvPht4;1 reduces arsenic translocation from roots to shoots in tobacco plants. Environ. Sci. Technol. 54, 1045–1053. https://doi.org/10.1021/acs.est.9b05486.

Sun, L., Song, L., Zhang, Y., Zheng, Z., Liu, D., 2016. *Arabidopsis* PHL2 and PHR1 act redundantly as the key components of the central regulatory system controlling transcriptional responses to phosphate starvation. Plant Physiol. 170, 499–514. https://doi.org/10.1104/pp.15.01336.

Tu, C., Ma, L.Q., Zhang, W.H., Cai, Y., Harris, W.G., 2003. Arsenic species and leachability in the fronds of the hyperaccumulator Chinese brake (Pteris vittata L.). Environ. Pollut. 124, 223–230. https://doi.org/10.1016/S0269-7491(02)00470-0.

Villadangos, A.F., Fu, H.L., Gil, J.A., Messens, J., Rosen, B.P., Mateos, L.M., 2012. Efflux permease CgAcr3-1 of *Corynebacterium glutamicum* is an arsenite-specific antiporter. J. Biol. Chem. 287, 723–735. https://doi.org/10.1074/jbc.M111.263335.

Wan, X., Yang, J., Lei, M., 2018. Speciation and uptake of antimony and arsenic by two populations of *Pteris vittata* L. and *Holcus lanatus* L. from co-contaminated soil. Environ. Sci. Pollut. Res. 25, 32447–32457. https://doi.org/10.1007/s11356-018-3228-z.

Wang, C., Na, G.N., Bermejo, E.S., Chen, Y., Banks, J.A., Salt, D.E., Zhao, F.-J., 2018. Dissecting the components controlling root-to-shoot arsenic translocation in *Arabidopsis thaliana*. New Phytol. 217, 206–2018. https://doi.org/10.1111/nph.14761.

Wang, H.B., Xie, F., Yao, Y.-Z., Zhao, B., Xiao, Q.-Q., Pan, Y.-H., Wang, H.-J., 2012. The effects of arsenic and induced-phytoextraction methods on photosynthesis in *Pteris* species with different arsenic-accumulating abilities. Environ. Exp. Bot. 75, 298–306. https://doi.org/10.1016/j.envexpbot.2011.08.002.

Wysocki, R., Bobrowicz, P., Ulaszewski, S., 1997. The *Saccharomyces cerevisiae* ACR3 gene encodes a putative membrane protein involved in arsenite transport. J. Biol. Chem. 272, 30061–30066. https://doi.org/10.1074/jbc.272.48.30061.

Yan, H.L., Gao, Y.W., Wu, L.L., Wang, L.Y., Zhang, T., Dai, C.H., Xu, W.X., Feng, L., Ma, M., Zhu, Y.G., He, Z.Y., 2019. Potential use of the *Pteris vittata* arsenic hyperaccumulation-regulation network for phytoremediation. J. Hazard. Mater. 368, 386–396. https://doi.org/10.1016/j.jhazmat.2019.01.072.

Yang, C.Y., Ho, Y.N., Makita, R., Inoue, C., Chien, M.F., 2020. *Cupriavidus basilensis* strain r507,a toxic arsenic phytoextraction facilitator, potentiates the arsenic accumulation by *Pteris vittata*. Ecotoxicol. Environ. Saf. 190, 110075 https://doi.org/10.1016/j.ecoenv.2019.110075.

Zemanová, V., Pavlíková, D., Dobrev, P.I., Motyka, V., Pavlík, M., 2019. Endogenous phytohormone profiles in Pteris fern species differing in arsenic accumulating ability. Environ. Exp. Bot. 166, 103822 https://doi.org/10.1016/j.envexpbot.2019.103822.

Zemanová, V., Popov, M., Pavlíková, D., Kotrba, P., Hnilička, F., Česká, J., Pavlík, M., 2020. Effect of arsenic stress on 5-methylcytosine, photosynthetic parameters and nutrient content in arsenic hyperaccumulator *Pteris cretica* (L.) var. *Albo-lineata*. BMC Plant Biol. 20, 130. https://doi.org/10.1186/s12870-020-2325-6.

Zhang, X.M., Yang, X.Y., Wang, H.B., Li, Q.C., Wang, H.J., Li, Y.Y., 2017. A significant positive correlation between endogenous trans-zeatin content and total arsenic in arsenic hyperaccumulator *Pteris cretica* var. *Nervosa*. Ecotoxicol. Environ. Saf. 138, 199–205. https://doi.org/10.1016/j.ecoenv.2016.12.031.

Zhao, F.J., Wang, J.R., Barker, J.H.A., Schat, H., Bleeker, P.M., McGrath, S.P., 2003. The role of phytochelatins in arsenic tolerance in the hyperaccumulator *Pteris vittata*. New Phytol. 159, 403–410. https://doi.org/10.1046/j.1469-8137.2003.00784.x.